Journal of Neuroscience Research 72:393–404 (2003)

Differential Connexin Expression, Gap Junction Intercellular Coupling, and Hemichannel Formation in NT2/D1 Human Neural Progenitors and Terminally Differentiated hNT Neurons

Sherri Boucher and Steffany A.L. Bennett*

Neural Regeneration Laboratory, Department of Biochemistry, Microbiology, and Immunology, University of Ottawa, Ottawa, Ontario, Canada

Connexin-mediated gap junctions and open hemichannels in nonjunctional membranes represent two biologically relevant mechanisms by which neural progenitors can coordinate their response to changes in the extracellular environment. NT2/D1 cells are a teratocarcinoma progenitor line that can be induced to differentiate terminally into functional hNT neurons and NT-G nonneuronal cells. Clinical transplants of hNT neurons and experimental grafts of NT2/D1 progenitors or hNT neurons have been used in cell-replacement therapy *in vivo*. Previous studies have shown that NT2/D1 cells express connexin 43 (Cx43) and that NT2/D1 progenitors are capable of dye transfer. To determine whether NT2/D1 progenitors and differentiated hNT cultures express other connexins, Cx26, Cx30, Cx32, Cx36, Cx37, Cx43, and Cx46.6 mRNA and protein were analyzed. NT2/D1 progenitors express Cx30, Cx36, Cx37, and Cx43. hNT/NT-G cultures express Cx36, Cx37, and *de novo* Cx46.6. Cx26 and Cx32 were not expressed in NT2/D1 or hNT/NT-G cells. NT2/D1 progenitors formed functional gap junctions as assessed by dye coupling as well as open hemichannels in nonjunctional membranes as assessed by dye-uptake studies. Dye coupling was inhibited by the gap junction blocker 18α-glycyrrhetinic acid. Hemichannel activity was inhibited by the dual-specificity chloride channel/connexin hemichannel inhibitor flufenamic acid but not by the chloride channel inhibitor 4,4′-diisothiocyanatostilbene-2,2′-disulfonic acid. Both dye coupling and dye uptake were substantially reduced following differentiation of NT2/D1 progenitors. We conclude that the pattern of connexin expression in NT2/D1 cells changes over the course of differentiation corresponding with a reduction in biochemical coupling and hemichannel activity in differentiated cells.

Key words: connexin; hemichannel; gap junction; differentiation; progenitor

The human adult brain is extremely vulnerable to injury, and there are no therapies available to reverse neuronal loss. The recent discovery that the adult central nervous system (CNS) can support neural progenitor populations raises hope for therapeutic regeneration of damaged CNS tissue (Gage, 2000; Temple, 2001). Human NT2/D1 cells are a clonal human teratocarcinoma cell line that can be induced to differentiate into functional neurons (hNTs), astrocytes, and nonneuronal cells (NT-Gs) when treated with retinoic acid and mitotic inhibitors (Andrews et al., 1984; Pleasure et al., 1992; Bani-Yaghoub et al., 1999b; Baldassarre et al., 2000; Sandhu et al., 2002; Sodja et al., 2002). hNT neurons have been transplanted into adult brain as part of phase I clinical trials for treatment of stroke (Meltzer et al., 2001; Nelson et al., 2002). Experimental evidence has supported hNT grafts as a viable therapy for neurodegenerative disease (Hurlbert et al., 1999; Baker et al., 2000; Saporta et al., 2001; Willing et al., 2001; Garbuzova-Davis et al., 2002). Moreover, NT2/D1 progenitors, transplanted directly into the brain of nude mice, can successfully differentiate into both neuron-like and oligodendrocyte-like cells (Ferrari et al., 2000).

It is essential to understand how host CNS interacts with grafted progenitors and their progeny to promote transplant survival and functional integration. Targeting connexin (Cx)-mediated communication represents one potential means of altering neural progenitor fate *in vivo* and *in vitro*. Connexins are a highly related family of at least 20 human proteins that form the structural subunits of

*Correspondence to: Dr. Steffany Bennett, Neural Regeneration Laboratory, Department of Biochemistry, Microbiology, and Immunology, University of Ottawa, Ottawa, Ontario, Canada K1H 8M5.
E-mail: sbennet@uottawa.ca

Received 19 September 2002; Revised 8 November 2002; Accepted 19 December 2002

gap junction channels, some of which form hemichannels in nonjunctional membranes that may open under certain conditions (Harris, 2001; Willecke et al., 2001). Hexameric assemblies of connexins form connexons (hemichannels) anchored in the plasma membrane. Gated Cx32, Cx26, Cx43, and Cx45 hemichannels facilitate passage of metabolites and second messengers to and from extracellular space, thereby providing a biological mechanism by which cells can sample and respond to environmental changes (Castro et al., 1999; Kammermans et al., 2001; Stout et al., 2002; Valiunas, 2002). When connexons of adjacent cells align, they define a single axial channel linking two cells. Clustered assemblies of these channels form the morphologically defined gap junction (Bruzzone et al., 1996). Cells coupled by gap junctions synchronize their responses to extracellular cues by the exchange of ions, metabolites, and second messengers (<1 kD; Bruzzone et al., 1996), representing one mechanism by which neural progenitors can synchronize their survival, differentiation, and deletion in response to environmental cues (Lo Turco and Kriegstein, 1991; Peinado et al., 1993b).

In this study, we characterized connexin expression in NT2/D1 cells and show, for the first time, that these cells are capable of forming functional connexin-mediated hemichannels in nonjunctional membranes. Previous studies have shown that NT2/D1 cells form functional gap junctions and express Cx43 (Andrews et al., 1984; Bani-Yaghoub et al., 1997). To identify a wider repertoire of CNS connexins in NT2/D1 cells, we evaluated Cx26, Cx30, Cx32, Cx36, Cx37, Cx43, and Cx46.6 at the mRNA and protein levels. We demonstrate that, in addition to Cx43, NT2/D1 progenitors express Cx30, Cx36, and Cx37. Following retinoic acid-induced differentiation, *de novo* Cx46.6, and a substantial decrease in Cx43 expression are observed. Furthermore, both gap junction intercellular communication (GJIC) and inducible hemichannel activity in NT2/D1 progenitors are reduced following terminal differentiation.

MATERIALS AND METHODS

Cell Culture

All chemical reagents were obtained from Sigma (St. Louis, MO), and all cell culture reagents were obtained from Invitrogen (Burlington, Ontario, Canada) unless otherwise stated. Passage 58–60 NT2/D1 cultures (Stratagene, La Jolla, CA) were maintained in Dulbecco's modified Eagle's medium (DMEM)/F-12 containing 10% fetal bovine serum (FBS), 1% penicillin/streptomycin, and 2 mM L-glutamine at 37°C in a 5% CO_2/95% air atmosphere. In differentiation studies, 2×10^6 cells were seeded in 75-cm^2 flasks and treated with 10 μM retinoic acid three times per week for 4 weeks. After retinoic acid treatment, the cells were replated 1:3. The conditioned medium was removed 48 hr after plating, and cells were replated at 1×10^7 cells per 10-cm^2 plate on poly-D-lysine (100 μg/ml)/laminin (20 μg/ml)-coated plates in a 1:1 mix of DMEM/F-12 and conditioned media. Cultures were supplemented with 1 μM cytosine β-D-arabinofuranoside (Sigma) and 10 μM 5-fluoro-2′-deoxyuridine (Sigma) mitotic inhibitors for 4 days. Cells were subsequently fed every 4 days for a minimum of 3 weeks with DMEM/F-12 containing 1 μM cytosine arabinoside, 10 μM fluorodexoyuridine, and 10 μM uridine (Sigma). Mitotic inhibitors were removed 24 hr prior to experimentation.

TABLE I. Human-Specific Connexin PCR Primer Pair Sequences and Amplicon Sizes

Human Cx gene	Strand	Primer sequence (5′-3′)	Amplicon size (bp)
Cx26	Sense	CTGCAGCTGATCTTCGTGTC	308
	Antisense	AAGCAGTCCACAGTGTTG	
Cx30	Sense	GTGACGAGCAAGAGGACTTC	512
	Antisense	CAGCAGCAGGTAGCACAACT	
Cx32	Sense	CTGCTCTACCCGGGCTATGC	750
	Antisense	ACGGCTGAGCATCGGTCGCTCTT	
Cx36	Sense	AACGCCGCTACTCTACAGTC	596
	Antisense	CCTTGGCAGGTCCTTGTTAC	
Cx37	Sense	ATCTGGCTGACGGTGCTCTT	619
	Antisense	GCACCAACTCCAGCAGGTTA	
Cx43	Sense	CTCAGCAACCTGGTTGTGAA	709
	Antisense	TCGCCAGTAACCAGCTTGTA	
Cx46.6	Sense	GACGAGCAGGCCAAGTTCAC	572
	Antisense	ACCTCGAAGCCGTACAGCAG	

Reverse Transcriptase-Polymerase Chain Reaction Analysis of Connexin Expression

All reagents were obtained from Invitrogen unless otherwise stated. Total RNA was isolated from cultured cells using the Trizol reagent according to the manufacturer's recommendations. RNA template was treated with DNaseI (Promega, Madison, WI) to eliminate residual genomic DNA. First-strand cDNA synthesis was performed using random hexamers (Promega) and Superscript II RT according to the manufacturer's recommendations. The resulting random-primed cDNA template was used to determine expression of several human connexin genes by PCR (Table I). The following reagents were added to each PCR: 25 pmoles forward primer, 25 pmoles reverse primer, 5 μl 10× PCR buffer, 4 μl 10 mM deoxynucleotide triphosphates (dNTPs; Promega), and 1 mM $MgCl_2$. The PCR was brought up to a final volume of 50 μl with nuclease-free water (Promega) and amplified in the GeneAmp PCR System 2400 (Applied Biosystems, Foster City, CA) using the standard protocol: 94°C for 5 min, 30–35 cycles of 94°C for 30 sec, 55°C for 60 sec, and 72°C for 2 min, and a final incubation at 72°C for 7 min. Amplification of Cx30, Cx36, and Cx46.6 required modifications. For Cx30, the PCR included 10 pmoles of both forward and reverse primers, 1.5 mM $MgCl_2$, 7.5% dimethyl sulfoxide (DMSO), and 1.5 μl Taq DNA polymerase. The annealing temperature was adjusted to 53°C for 30 sec; extension time was reduced to 45 sec. For Cx36, the annealing temperature was adjusted to 50°C. For Cx46.6, 7.5% DMSO, 1.5 μl Taq DNA polymerase was added to the PCR mix. The annealing temperature was adjusted to 61°C for 30 sec; extension time was reduced to 45 sec.

Western Analysis

NT2/D1 and hNT/NT-G protein for each culture were isolated in RIPA buffer [1% Nonidet P-40, 0.5% sodium de-

oxycholate, 0.1% sodium dodecyl sulfate (SDS), 1 mM NaF, 50 μg/ml apoprotin, 1 mM sodium orthovanadate, 1 mg/ml phenylmethylsulfonyl fluoride, 10 mM phosphate-buffered saline (PBS)] or Trizol reagent (Invitrogen). As a positive control, protein was isolated from human hippocampal tissue obtained from the Montreal Brain Bank (Montreal, Quebec, Canada). Protein concentration was determined using the Bio-Rad DC protein assay kit (Bio-Rad, Hercules, CA). All chemicals were from Sigma except where indicated. Protein samples (30 μg) were separated by SDS-polyacrylamide gel electrophoresis (SDS-PAGE) under denaturing conditions and transferred to a polyvinylidene difluoride (PVDF) membrane (Fisher Scientific, Nepean, Ontario, Canada). Membranes were blocked in 10 mM PBS containing 1% casein. Primary antibodies were diluted in the same solution. Dilutions were as follows: mouse anti-Cx30 (Zymed, San Francisco, CA; 1 μg/ml), rabbit anti-Cx36 (C-terminus; Zymed; 5 μg/ml), mouse anti-Cx37 (Alpha Diagnostics, San Antonio, TX; 10 μg/ml), rabbit anti-Cx43 (Chemicon, Mississauga, Ontario, Canada; 1:300). Secondary antibodies were peroxidase-conjugated anti-mouse IgG (Jackson Immunoresearch, West Grove PA; 1:2,000) or peroxidase-conjugated anti-rabbit IgG (Jackson Immunoresearch; 1:5,000). For Cx37 immunoblots, tertiary enhancement was required. Blots were incubated with biotinylated anti-mouse IgG (Sigma; 1:10,000) and extravidin peroxidase (Sigma; 1:1,000). Cx37 immunoblots were reprobed with anti-β-tubulin (Sigma; 1:300). Immunoreactivity was visualized by enhanced chemiluminescence using the SuperSignal West Pico Chemiluminescent Substrate kit (MJS BioLynx Inc., Brockville, Ontario, Canada). All other details are as described by Bennett et al. (2000).

Immunocytochemistry

Undifferentiated NT2/D1 cells were maintained as described above. For analysis of hNT/NT-G cultures, cells were differentiated as described and plated into dishes containing glass coverslips coated with poly-D-lysine (100 μg/ml)/laminin (20 μg/ml) prior to commencing mitotic inhibition. Cultures were fixed in cold 3.7% formaldehyde in 10 mM PBS (2.5 mM monobasic sodium phosphate, 7.5 mM dibasic sodium phosphate, 154 mM NaCl, pH 7.2) for 10 min followed by incubation in 100% methanol for 3 min. Primary antibodies were antineuron-specific enolase (Calbiochem, LaJolla, CA; 1:500), mouse anti-Cx30 (Zymed; 5 μg/ml), rabbit anti-Cx36 (Zymed; 1 μg/ml), mouse anti-Cx37 (Alpha Diagnostics; 1 μg/ml), and rabbit anti-Cx43 (Chemicon; 1:1000). Secondary antibodies were Cy3-conjugated anti-mouse (Jackson Immunoresearch; 1:800). Fluorescein isothiocyanate (FITC)-conjugated anti-mouse (Jackson Immunoresearch; 1:100), or Cy3-conjugated anti-rabbit (Jackson Immunoresearch; 1;600) IgG. Antibodies were diluted in Ab buffer (10 mM PBS, 0.3% Triton X-100, 3% bovine serum albumin). Cells were coverslipped with Vectashield (Vector Laboratories Inc., Burlingame, CA), sealed, and visualized on a Leica DMRXA2 epifluorescent microscope (Leica, Longueuil, Quebec, Canada). Because suppliers did not provide verification of antibody reactivity with human antigen, optimal dilutions were established by immunoperoxidase labeling of 4 μM paraffin-embedded sections of human hippocampal sections. Tissue was obtained from the Montreal Brain Bank. All other details were as described by Bennett et al. (1998, 2000).

Gap Junction Fluorescent Dye Transfer

Biochemical coupling associated with GJIC was assessed by dye transfer. NT2 cells were grown to 100% confluence. hNT/NT-G cultures were differentiated as described above. Cells were washed twice with 10 mM PBS and incubated for 1 min with lucifer yellow (LY; 1 mg/ml)/rhodamine B isothiocyanate-dextran (RD; 1 mg/ml) solution or LY/RD solution containing 100 μM 18α-glycyrrhetinic acid (αGA). Cells were scraped gently with a syringe needle and incubated at room temperature for an additional 3 min. After incubation, cells were washed twice with 10 mM PBS and fixed as described above. All dye-transfer assays were performed on triplicate cultures, with $n = 5$ transfer assays per experiment, for a total of $n = 15$ measurements/condition. In NT2/D1 assays, dye transfer was quantified by measuring the distance of LY transfer from the scrape line. Cells positive for both LY and RD were excluded from measurements to control for LY uptake resulting from loss of cell membrane integrity. To establish specificity, the mean LY transfer distance in untreated cells was set to 100% and dye transfer in the presence of the GJIC inhibitor was standardized to this value. Data are expressed as mean ± standard error of measurement (SEM). In hNT/NT-G assays, the number of LY^+/RD^- cells along the scrape line was established using serial photographs taken along the entire length of the scrape (9–14 photos/coverslip) on triplicate cultures to assess accurately GJIC in hNT aggregates, single neurons, and nonneuronal NT-Gs. Two coverslips were assessed per culture for a total of $n = 54–84$ measurements per condition. Data are expressed as the mean number of LY^+/RD^- cells ± SEM. Statistical data were subject to one-way analysis of variance (ANOVA), followed by *post hoc* Dunnett's *t*-test, with a confidence level of 95%.

Detection of Transmembrane Dye Flux Through Open Hemichannels

Transmembrane flux of LY but not RD into cells was used to detect open hemichannels as described by Stout et al. (2002). NT2/D1 cells were grown at low density sufficient to visualize independent colonies. Cells were washed with 10 mM PBS and coated with LY/RD solution in the presence and absence of glass microbeads alone or in combination with 50 μM flufenamic acid (FFA) or 100 μM 4,4′-diisothiocyanatostilbene-2,2′-disulfonic acid (DIDS) as described by Stout et al. (2002). Cells were incubated for 3 min at room temperature. After incubation, cells were washed twice with 10 mM PBS and fixed as described above. Replicate experiments were performed for each condition. For quantitation, 16–20 random fields were taken per condition, and the number of LY^+/RD^- cell colonies not in contact with adjacent colonies was counted, for a total of 32–40 measurements/condition. Cells positive for both LY and RD were excluded from quantitation to control for LY uptake resulting from loss of cell membrane integrity. For NT2/D1 assays, the number of LY^+/RD^- cells is expressed as a percentage of the total number of cells per colony per microscopic field. Because subconfluent cultures cannot be obtained for hNT/NT-G cultures, absolute values for the number of LY^+/RD^- cells were used as quantitative measurements of open hemichannels. For statistical anal-

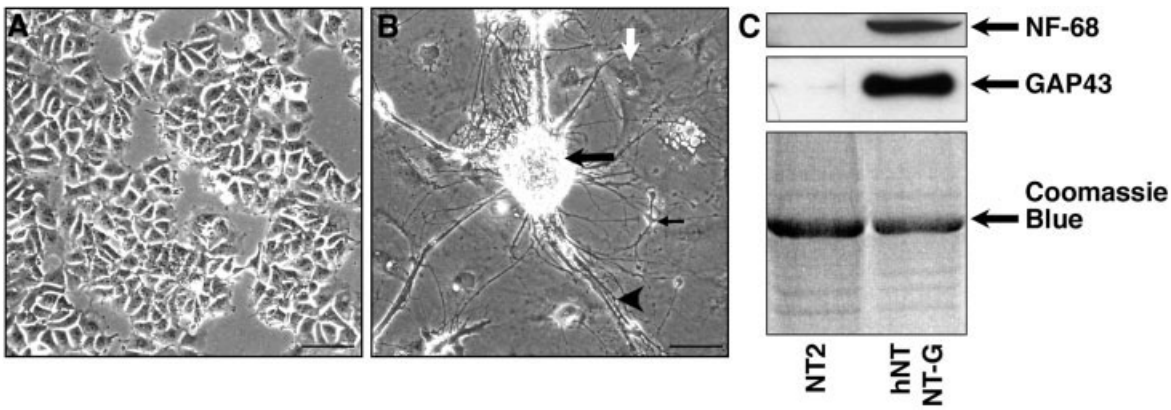

Fig. 1. NT2/D1 can be terminally differentiated into hNT/NT-G cells by sequential treatment with retinoic acid and mitotic inhibitors. **A:** Undifferentiated NT2/D1 cells. **B:** Differentiated hNT neurons (small black arrow) with extensive neurites (arrowhead) are often aggregated into large clusters (large black arrow) on top of a feeder layer of adherent flat cells (white arrow) **C:** NF68 and GAP43 are expressed by hNT/NT-G cultures but not NT2/D1 cultures. Because both actin and β-tubulin levels (see Fig. 5A) change over the course of NT2/D1 differentiation, loading controls were Coomassie blue-stained gels separating the same protein samples used for immunoblotting. Scale bars = 50 μm.

yses, results were subjected to one-way ANOVA, followed by *post hoc* Tukey test, with a confidence level of 95%.

RESULTS

NT2/D1 Differentiate to hNT Neurons and NT-G Nonneuronal Cells Following Retinoic Acid Treatment

Morphological changes associated with terminal differentiation of NT2/D1 cells have been well documented (Pleasure et al., 1992), and these features were replicated in the present study (Fig. 1). After 4 weeks of retinoic acid treatment and 3 weeks of mitotic inhibition, cultures contained cells with two distinct morphologies (Fig. 1B). hNT neurons, with refractile, small cell bodies (small black arrow) interconnected by extensive neuritic outgrowth (arrowhead) and often aggregated into tightly packed bundles (large black arrow); could be seen growing on top of a feeder layer of large, adherent flat cells (white arrow; Fig. 1B). Western analysis confirmed neuronal differentiation (Figs. 1C, 5A). hNT/NT-G cultures but not NT2/D1 progenitors expressed neurofilament 68 (NF-68; a 68-kD marker of differentiated neurons; Fig. 1C), growth-associated protein 43 (GAP43; a 43-kD marker of neurons undergoing neuritic extension; Fig. 1C), and β-tubulin isotype III (a 50–55-kD marker of CNS neurons and glia; Fig. 5A). Immunocytochemistry and quantitation of neuron-specific-enolase$^+$/vimentin$^-$ and enolase$^-$/vimentin$^+$ cells were performed to establish culture composition. Triplicate hNT/NT-G cultures, differentiated at the same time as cultures used for molecular and biochemical analyses, were composed of 86% ± 4.8% hNT neurons (mean ± SEM) and 14% ± 4.8% NT-G nonneuronal cells.

NT2/D1 Progenitors Express Cx30, Cx36, Cx37, and Cx43 but Not Cx26, Cx32, or Cx46.6 mRNA

RT-PCR analysis detected Cx30, Cx36, Cx37, and Cx43 transcript in triplicate NT2/D1 cultures (Fig. 2A; NT2 + RT). Cx26, Cx32, and Cx46.6 were not expressed in NT2/D1 cells (Fig. 2A; NT2 + RT). The same random-primed RT products were amplified with GAPDH to demonstrate template integrity (Fig. 2B; GAPDH).

hNT/NT-G Cultures Express Cx36, Cx37, and Cx46.6 mRNA

Total RNA from triplicate cultures was subjected to RT-PCR analysis (Fig. 2). All of the hNT/NT-G cultures tested expressed Cx43, Cx36, and Cx46.6 but not Cx26 or Cx32 (Fig. 2A; hNT + RT). An increase in mRNA expression of Cx36 and a decrease in mRNA expression of Cx43 relative to NT2/D1 expression were consistently observed. Cx37 was detected in two of three cultures (Fig. 2A; hNT + RT). Cx30 was detected in one of three hNT/NT-G cultures. The same random-primed RT products were amplified with GAPDH to demonstrate template integrity (Fig. 2B).

Sequence Verification of Cx46.6

The Cx46.6 sequence in the GenBank database (NCBI; www.ncbi.nim.nih.gov) is a virtual human connexin gene and has not been empirically demonstrated in human CNS prior to this study. It was originally predicted from NCBI contig NT 004908 by automated computational analysis using the gene prediction method BLAST, supported by mRNA and human EST evidence (see Genbank GI: 11427877, submitted by B.K. Bloemker, A. Swaroop, and W.J. Kimberling). The predicted protein sequence for Cx46.6 is 436 amino acids in length (GI:

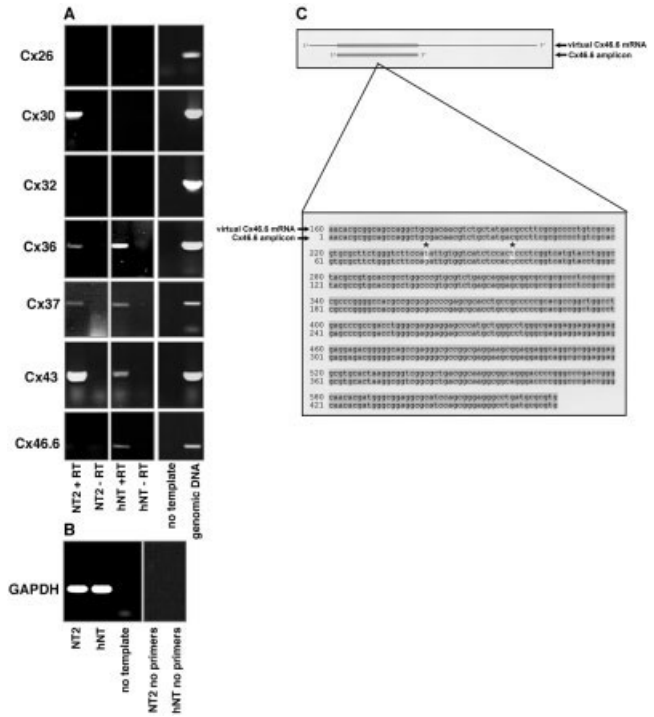

Fig. 2. NT2/D1 and hNT/NT-G cultures express mRNAs for multiple connexins present in the mammalian central nervous system. **A:** RT-PCR analysis of random-primed total RNA from NT2/D1 and mixed hNT/NT-G cultures. Cx30, Cx36, Cx37, and Cx43 mRNAs were present in all NT2/D1 cultures tested (NT2 + RT). Cx36, Cx43, and Cx46.6 mRNA were present in all hNT cultures tested (hNT + RT). Cx30 and Cx37 mRNAs were present in 1/3 and 2/3 of hNT cultures tested (hNT + RT). **B:** cDNA templates were confirmed using GAPDH as an internal standard (GAPDH). Controls included RT reactions performed without the addition of reverse transcriptase enzyme (−RT) and PCR performed without cDNA template (no template) or primers (no primers) to detect genomic DNA contamination, reagent contamination, and PCR artifact respectively. NT2 genomic DNA was used as a positive PCR control (genomic DNA). **C:** Alignment of the virtual Cx46.6 mRNA sequence (GI: 11427877) and the sequenced Cx46.6 hNT/NT-G PCR product. This amplicon sequence was 99% homologous to the virtual mRNA sequence with two base pair mismatches (asterisks).

27385777). In 2001, Teubner *et al.* reported neuronal expression of a new mouse connexin designated Cx47 (Teubner et al., 2001), although it now appears that Cx47 is more likely expressed in myelinating cells (Altevogt et al., 2002). To identify murine Cx47, the sequence of the Cx46.6 virtual human connexin gene was combined with rat EST data to generate a PCR probe used to screen and clone mCx47 from a mouse genomic DNA library (Teubner et al., 2001). Together, the cloning approach and the expression pattern of the mouse Cx47 gene suggested that "virtual" Cx46.6 is an actual human connexin gene likely expressed in human CNS. Therefore, Cx46.6 was included in the battery of connexin genes investigated in the NT2/D1 cell line. To verify the identity of the hNT/NT-G amplicon, the 572-bp Cx46.6 PCR fragment was subjected to direct sequencing in both forward and reverse orientations. Alignment produced a high-quality 468-bp sequence. This sequence was 99% homologous to the virtual Cx46.6 sequence with two base pair mismatches (Fig. 2C, asterisks).

Connexin Protein Expression and Localization in NT2/D1 and hNT/NT-G Cultures

To confirm connexin expression at the protein level, immunocytochemical and immunoblot analyses for Cx30, Cx36, Cx37, and Cx43 were performed on triplicate NT2/D1 and hNT/NT-G cultures. The Cx43 antibody employed has been shown to detect human protein (Duffy et al., 2000). To verify reactivity of anti-Cx37, anti-Cx36, and anti-Cx30, human hippocampal tissue was first tested as a positive control. Cx30 was not detected in the positive control by Western blot or immunohistochemistry and was dropped from further evaluation. In all experiments, negative controls included NT2/D1 and hNT/NT2-G cells processed in the absence of primary antibody (Figs. 3, 4).

The predominant Cx43 isoforms in NT2/D1 cells were detected at 42–44 kD (Fig. 3A), suggestive of the phosphorylated forms of Cx43 (Bani-Yaghoub et al., 1999c). By immunocytochemistry, typical punctate gap junction staining localizing to plasma membranes between adjacent cells was observed (Fig. 3B,C arrows). Substantial perinuclear staining was also evident (Fig. 3B,C, arrowheads). A marked decrease in Cx43 protein was noted in hNT/NT-G cultures. By immunocytochemistry, low levels of protein could be detected at the plasma membrane of some large nonneuronal NT-G feeder (arrows) cells but not in hNT neurons (Fig. 3D,E). Cx43 was undetectable by Western analysis in hNT/NT-G protein (Fig. 3A).

Comparable levels of Cx36 protein were detected in both NT2/D1 and hNT/NT-G cultures (Fig. 4). Western blot analyses detected two bands at 36 kD and 66 kD (Fig. 4K) corresponding to the Cx36 dimer and monomer previously characterized using this antibody (Rash et al., 2000). Protein was localized to contiguous regions of plasma membrane between opposing NT2/D1 cells (Fig. 4A–D, arrows). In hNT/NT-G cultures, strong Cx36 immunoreactivity was observed in discrete cells in aggregated neuronal bundles (Fig. 4E,F). At higher magnification, strong punctate staining was detected between hNT cell soma (Fig. 4G,H, arrows). In addition to localization to hNT neurons, some nonneuronal NT-G cells in close apposition expressed Cx36 (Fig. 4I,J, arrows).

Reactivity of the Cx37 antibody with human Cx37 was confirmed by Western blot analysis of human hippocampal protein (Fig. 5). A doublet was detected in hippocampal lysates migrating at approximately 36 kD and 38 kD (Fig. 5A). This pattern is suggestive of the unphosphorylated and phosphorylated forms of Cx37 previously reported (Traub et al., 1998; Larson et al., 2000). The higher Cx37 band was detected at extremely low levels in both NT2/D1 and hNT/NT-G cultures (Fig. 5A). Cx37 was not observed in NT2/D1 cells by immunofluorescence (Fig. 5B,C), hNT neuronal bundles, or large NT-G feeder cells (Fig. 5D,E). Punctate immunoreactivity was

noted at the cell soma and in processes of morphologically distinct NT-G cells (Fig. 5F,G, arrows).

NT2/D1 but Not hNT/NT-G Cultures Are Capable of Dye Transfer Indicative of Intercellular Coupling

Functional connexin expression was assessed by dye transfer assays (Fig. 6). Biochemical coupling indicated by intercellular dye was detected in NT2/D1 cultures, with a mean LY^+/RD^- dye transfer distance of 145 ± 4 μm (Fig. 6A–C,J). Specificity was confirmed by the average 70% reduction in LY^+/RD^- dye transfer observed overall in the presence of the gap junction channel blocker αGA (Fig. 6D–F,J). Little to no LY dye transfer was observed in hNT/NT-G cultures. Dye coupling in the rare cells that were LY^+/RD^- was not affected by αGA treatment (Fig. 6G–I,K).

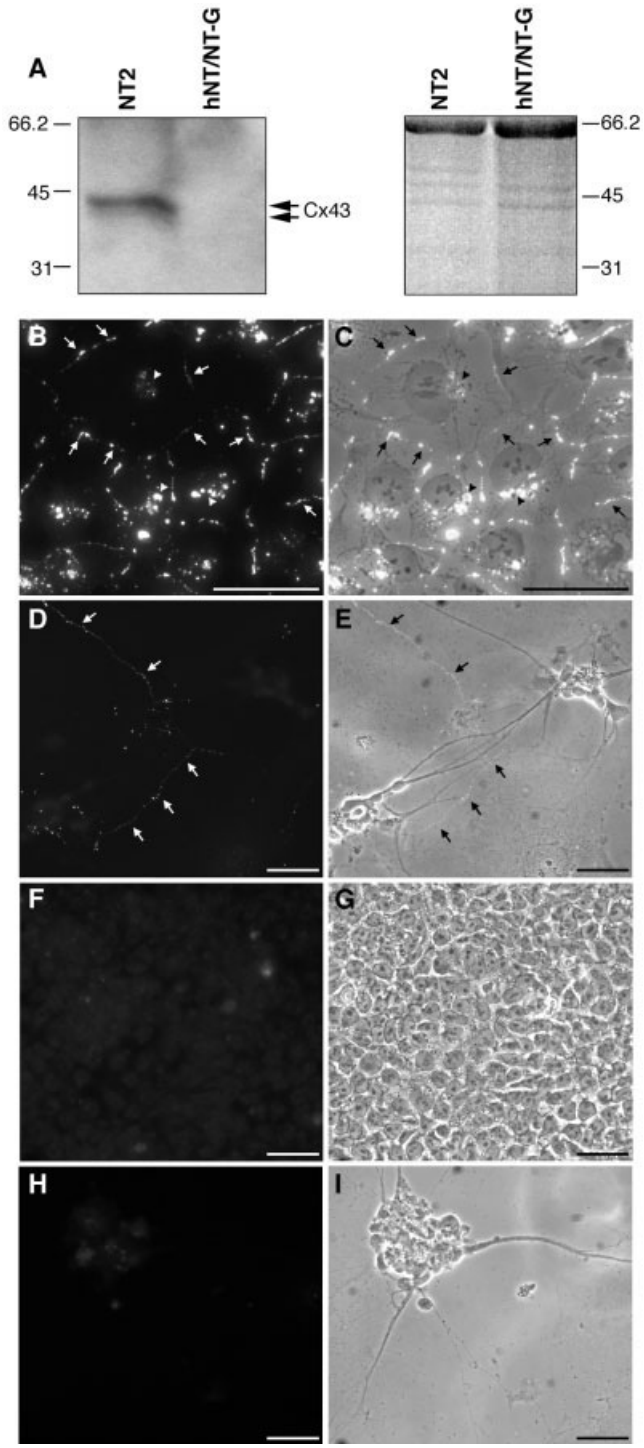

Fig. 3. Immunofluorescent localization and Western analysis of Cx43 in NT2/D1 and hNT/NT-G cultures. **A:** A doublet was observed in NT2/D1 cells by Western analysis at 42–44 kD (left panel). Loading controls were Coomassie blue-stained gels separating the same protein samples used for immunoblotting (right). **B:** Punctate Cx43 immunoreactivity was detected at the plasma membrane of adjacent NT2/D1 cells (arrows) as well as strong perinuclear labeling (arrowheads). **C:** Double exposure of phase-contrast and Cx43 immunofluorescence. **D:** A decrease in both the intensity of Cx43 immunoreactivity and the frequency of immunopositive cells was observed in hNT/NT-G cultures. Cx43 was localized to the plasma membrane of large, flat NT-G feeder cells (arrows) and was not detected in hNT neurons. **E:** Double exposure of phase-contrast and Cx43 immunofluorescence. **F:** NT2/D1 negative control processed in the absence of primary antibody. **G:** Phase-contrast of the NT2/D1 negative control. **H:** hNT/NT-G negative control processed in the absence of primary antibody. **I:** Phase-contrast of the hNT/NT-G negative control. Scale bars = 50 μm.

NT2/D1 but Not hNT/NT-G Cultures Form Functional Connexin-Mediated Hemichannels Capable of Dye Uptake

Transmembrane flux of LY but not RD into cells was used to identify the presence of open connexin-mediated hemichannels in nonjunctional membranes. Representative photomicrographs from dye-uptake assays in NT2/D1 cells are depicted in Figure 7. Spontaneous open hemichannel activity was extremely low (Fig. 7A,B; untreated − beads). A 17-fold increase in dye uptake was observed following mechanical stimulation with glass microbeads (Fig. 6A,B;untreated + beads). Hemichannel activity was reduced 50% by addition of the dual-specificity chloride channel and connexin channel inhibitor FFA (Fig. 7A,B;+FFA/+beads). Dye uptake was unaffected by the chloride channel inhibitor DIDS (Fig. 7A,B;+DIDS/+beads). Dye-uptake assays were also performed with FFA or DIDS in the absence of glass microbeads to eliminate possible effects of these inhibitors under noninducing hemichannel conditions (Fig. 7A,B; +FFA/−beads, +DIDS/−beads). No significant spontaneous or inducible hemichannel activity was detected in hNT/NT-G cultures (Fig. 7C).

DISCUSSION

In the present study, we have expanded the known repertoire of connexins expressed by NT2/D1 cells and identified a new functional correlate for this expression. NT2/D1 cells express Cx30, Cx36, Cx37, and Cx43

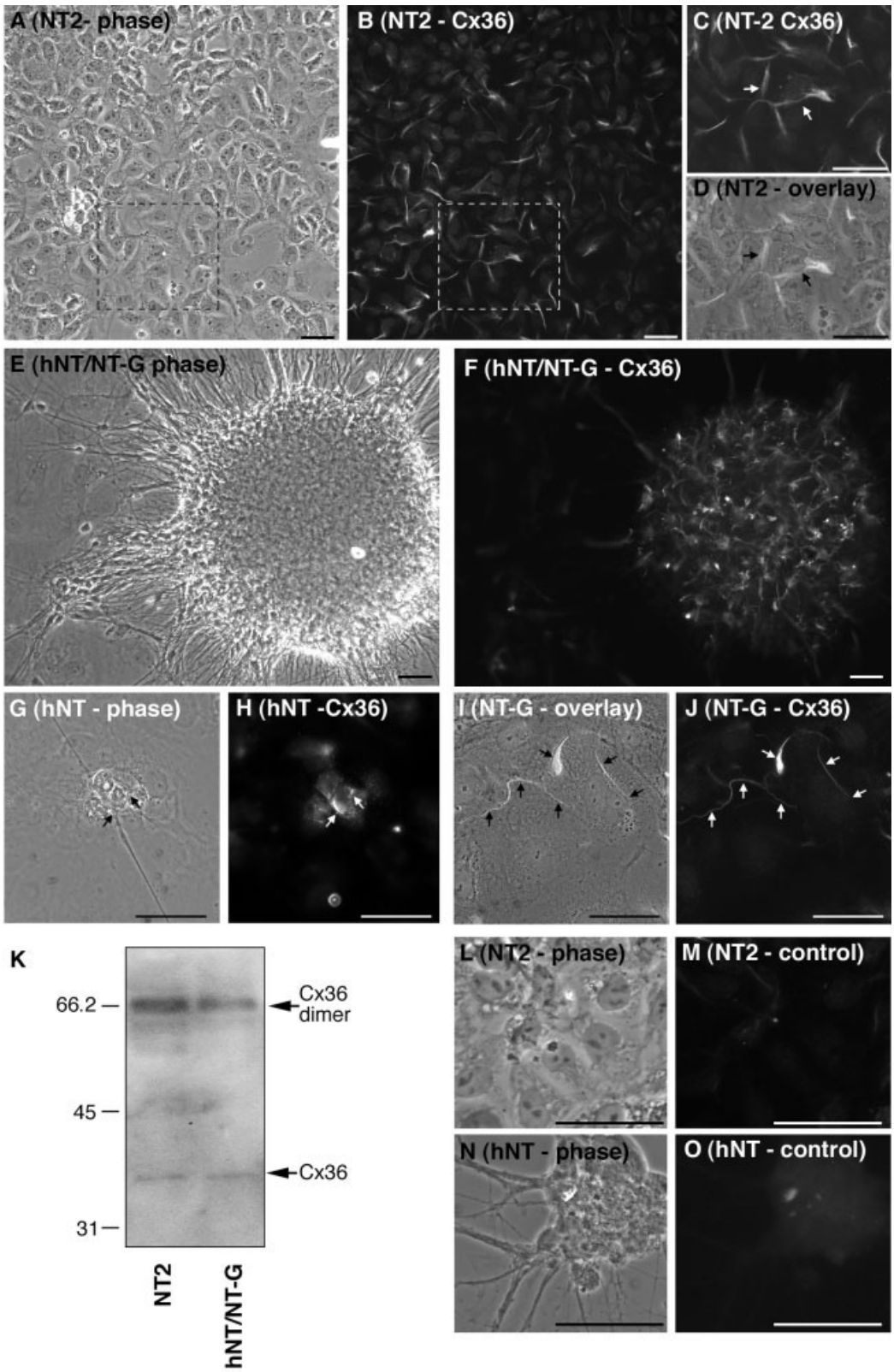

Fig. 4. Immunofluorescent localization and Western analysis of Cx36 in NT2/D1 and hNT/NT-G cultures. **A:** Phase-contrast of NT2/D1 cells. **B:** Cx36 immunofluorescence in NT2/D1 cells. **C:** Higher magnification of outlined area in A and B. **D:** Phase-contrast and immunofluorescent overlays. Note localization of Cx36 to the plasma membrane of adjacent NT2/D1 cells (arrows). **E:** Phase contrast of an hNT bundle on top of NT-G feeder cells. **F:** Cx36 immunofluorescence is localized primarily to hNT neurons. **G:** Phase contrast of hNT/NT-G cells. **H:** Cx36 immunofluorescence localizes to the plasma membrane of hNT neuronal soma (arrows). **I:** Phase-contrast and immunofluorescent overlays of NT-G cells. **J:** Cx36 immunofluorescence of NT-G cells. Strong immunoreactivity could be detected at the border between some NT-G cells. **K:** Two bands were observed in both NT2/D1 and hNT/NT-G cells at 36 kD and 66 kD. Loading controls of the same protein lysates are depicted in Figure 3 (right). **L–O:** Negative NT2/D1 and hNT/NT-G controls processed in the absence of primary antibody. Scale bars = 50 μm.

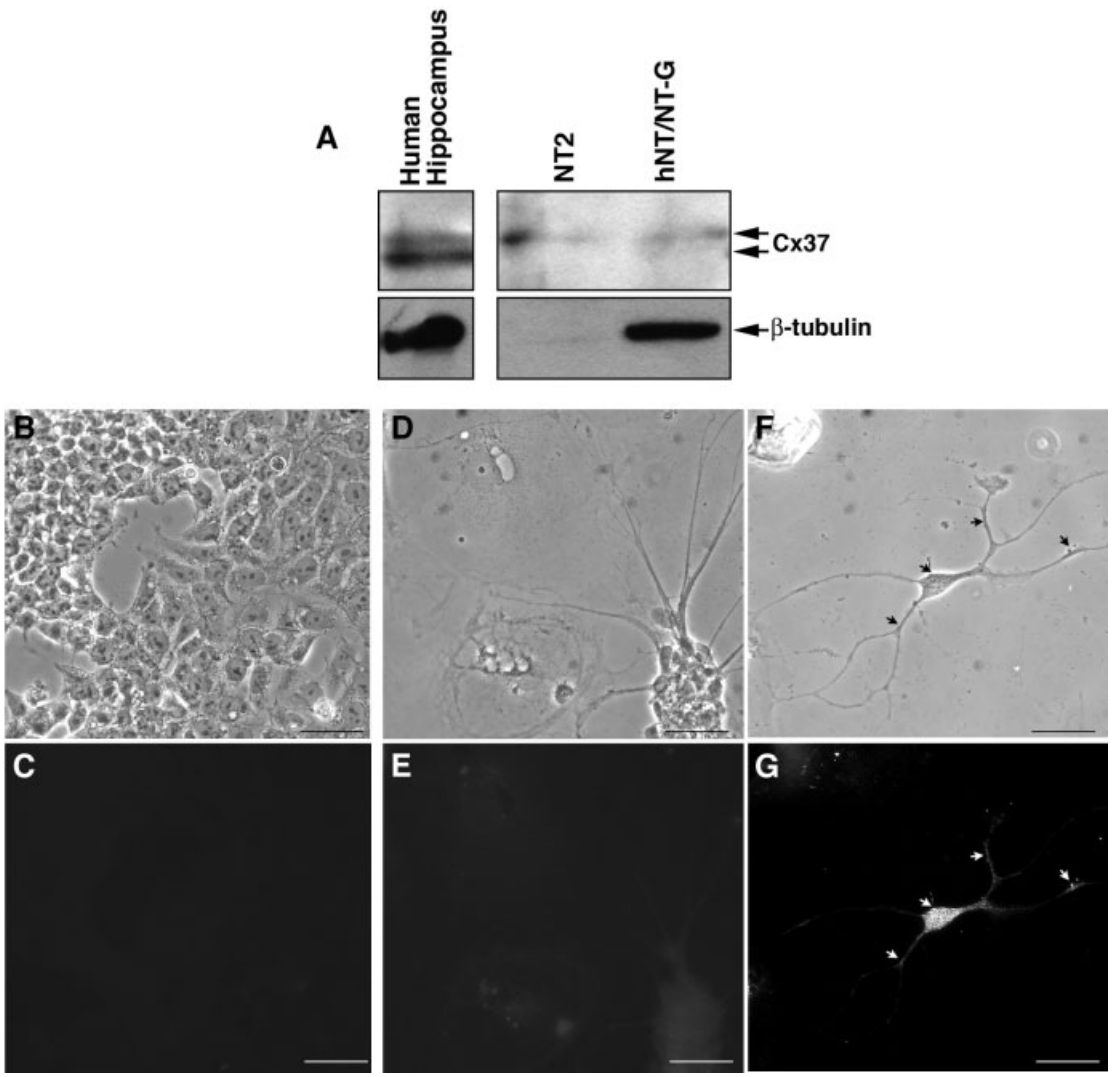

Fig. 5. Immunofluorescent localization and Western analysis of Cx37 in NT2/D1 and hNT/NT-G cultures. **A:** A doublet was observed in human hippocampus at 37–39 kD. Only the 39-kD band was detected at low levels in NT2/D1 and hNT/NT-G cells (top panel). Note that Western blotting required tertiary enhancement as described in Materials and Methods to detect Cx37. Loading controls of the same NT2/D1 and hNT/NT-G protein lysates are depicted in Figure 3 (right). The Cx37 immunoblot was stripped and probed for β-tubulin. An intense 50-kD band was detected in both human hippocampus and hNT/NT-G cells but not NT2/D1 cells. **B:** Phase contrast of NT2/D1 cells. **C:** Cx37 immunoreactivity was not detected in NT2/D1 cells. **D:** Phase contrast of an hNT bundle and NT-G feeder cells. **E:** Cx37 immunoreactivity was not detected in hNT neurons or large, flat NT-G feeder cells. **F:** Phase contrast of an NT-G cell immunopositive for Cx37. **G:** Strong punctate immunoreactivity was localized to some NT-G cell somas and, to a lesser extent along processes. Cells with this morphology were vimentin^{+} and enolase^{-}. Negative controls processed in the absence of primary antibody exhibited were identical to that shown in E. Scale bars = 50 μm.

mRNA, with confirmed protein expression of Cx36 and Cx43. Retinoic acid-differentiated hNT/NT-G cultures express Cx36, Cx37, and Cx46.6 mRNA, with confirmed protein expression of Cx36 and Cx37. Dye-transfer and uptake analyses indicate that NT2/D1 cells can form both functional gap junctions and open hemichannels in non-junctional membranes. Biochemical coupling and hemichannel activity are significantly reduced following terminal differentiation.

The significance of this study lies in accumulating evidence that connexin-mediated communication represents one means of influencing neural progenitor fate and commitment *in vitro* and *in vivo* (Guthrie and Gilula, 1989; Fulton, 1995; Bittman et al., 1997; Rozental et al., 1998, 2000; Bani-Yaghoub et al., 1999a; Bittman and LoTurco, 1999; Mercier and Hatton, 2001; Duval et al., 2002). hNT neuronal transplants have been used in experimental models of progressive neurodegeneration and are currently in

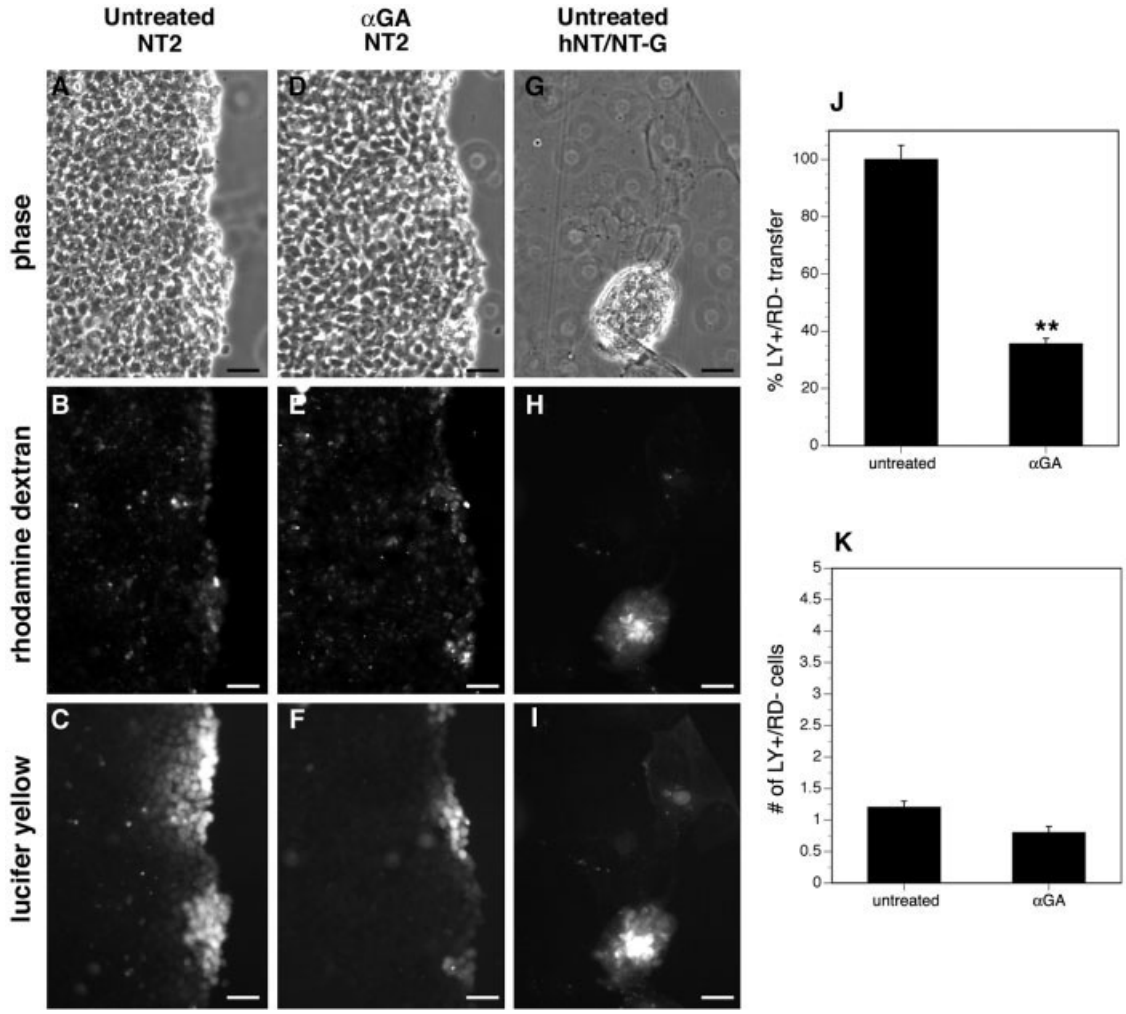

Fig. 6. Assessment of GJIC by scrape-loading dye transfer in NT2/D1 cells and hNT/NT-G cells. GJIC was assessed by LY/RD dye-transfer assays in triplicate NT2/D1 (**A–F,J**) and hNT-NT-G (**G–I,K**) cultures. RD^+ scrape-loaded NT2/D1 cells readily pass LY to adjacent cells (A–C,J; LY untreated). NT2/D1 dye transfer was inhibited by the gap junction blocker αGA (100 μM) (D–F,J; αGA; $^{**}P < 0.01$). Significant LY^+/RD^- dye transfer was not observed in any of the cell types in hNT/NT-G cultures (G–I,K). Scale bars = 50 μm.

phase 1 clinical trials for stroke therapy (Hurlbert et al., 1999; Baker et al., 2000; Meltzer et al., 2001; Saporta et al., 2001; Willing et al., 2001; Garbuzova-Davis et al., 2002; Nelson et al., 2002). Recently, direct grafting of NT2/D1 progenitors in rodent brain has been shown to result in functional differentiation in host CNS without detectable tumor formation (Ferrari et al., 2000). To improve survival, incorporation, and differentiation of exogenous progenitors and ensure safe, effective cell replacement, it is essential to be able to predict how NT2/D1, hNT neurons, and NT-G nonneuronal cells will interact with the host environment. Connexin-mediated GJIC and hemichannel formation in nonjunctional membranes represent two mechanisms by which neural progenitors may coordinate their survival, activation, and differentiation in adult CNS.

NT2/D1 cells have previously been shown to express Cx43 but not Cx26 or Cx32 (Bani-Yaghoub et al., 1997). Both Cx43 expression and GJIC as detected by dye transfer are down-regulated over the course of retinoic acid-induced differentiation (Bani-Yaghoub et al., 1997, 1999c). Our data are consistent with these studies. Moreover, we localize Cx43 protein to large, adherent nonneuronal cells with fibroblast-like morphology in hNT/NT-G cultures. Cx43 has been shown to be expressed in ependymal cells, leptomeningeal cells, and astrocytes in the mature CNS (Dermietzel and Spray, 1993; Nagy et al., 2001; Rash et al., 2001) and neural progenitors in the developing brain (Bittman et al., 1997; Bittman and LoTurco, 1999). Thus "flat cells" in hNT/NT-G cultures may represent leptomeningeal-like cells, glia, and/or immature neurons blocked in differentiation (Andrews et al.,

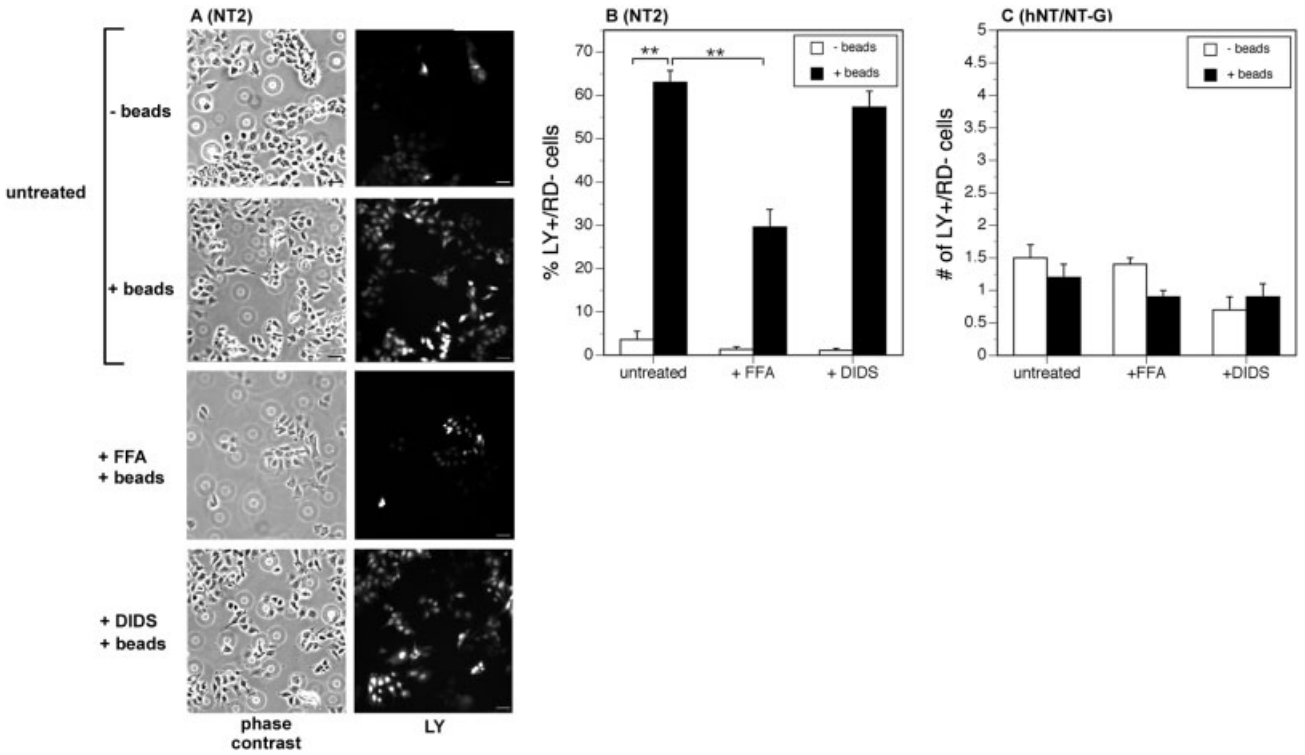

Fig. 7. Dye uptake through open connexin-mediated hemichannels in the plasma membrane is detected in NT2/D1 but not hNT/NT-G cells. Spontaneous LY uptake was observed at low levels in NT2/D1 cells (**A,B;** untreated). Open hemichannel activity could be induced by mechanical stimulation with glass microbeads (A,B; +beads; $^{**}P < 0.01$). Dye uptake was inhibited by the hemichannel/chloride channel inhibitor FFA (A,B; +beads/+FFA) but not the chloride channel inhibitor DIDS (A,B; +beads/+DIDS). No significant dye uptake was detected in any of the cell types in hNT/NT-G cultures (**C**). Scale bars = 50 μm.

1984; Pleasure et al., 1992; Bani-Yaghoub et al., 1999b; Sandhu et al., 2002; Sodja et al., 2002).

The present study adds further insight into how the reduction in biochemical coupling through gap junctions is achieved over the course of NT2/D1 differentiation (Bani-Yaghoub et al., 1997, 1999c). GJIC is widespread in the developing nervous system and is the predominant means of cell–cell communication prior to formation of chemical synapses (Lo Turco and Kriegstein, 1991; Peinado et al., 1993b). GJIC between progenitors and their progeny remains high during the first 2 weeks after parturition, corresponding with increased Cx36 and reduced Cx43 levels (Crain et al., 1973; Peinado et al., 1993a,b; Nadarajah et al., 1997; Peinado, 2001). A marked decrease in GJIC between committed neuronal progeny is observed, corresponding with a restriction in connexin expression to Cx36 and expression of Cx30, Cx26, Cx37, and Cx43 at astrocytic gap junctions (Rash et al., 2000, 2001; Nagy et al., 2001). This expression pattern is recapitulated *in vitro* in NT2/D1 progenitors and terminally differentiated hNT/NT-G cells. Cx30 mRNA and phosphorylated Cx37 were detected in NT2/D1 and in some, but not all, hNT/NT-G cultures. The ability of NT2/D1 cells to differentiate to neurons and astrocytes by altering concentrations of mitotic inhibitors following retinoic acid treatment has recently been reported (Bani-Yaghoub et al., 1999b; Sandhu et al., 2002). Given that our mixed cultures are composed of approximately 90% neurons and 10% nonneuronal cells, differential expression of Cx30 and Cx37 in hNT cultures may reflect variation in the identity of glial populations in hNT/NT-G cultures. Furthermore, the reduction in biochemical coupling as assessed by dye transfer is consistent with the loss of Cx43 and expression of Cx36 by terminally differentiated hNT neurons. Cx36 is one of the most selective of the connexins, with restricted permeability to anions and larger molecules (Srinivas et al., 1999; Teubner, 2000).

We also provide evidence for the presence of inducible connexin-mediated hemichannels capable of dye uptake in nonjunctional membranes of NT2/D21 progenitors but not terminally differentiated hNT/NT-G cultures. Spontaneous hemichannel activity was very low in NT2/D1 cells, suggesting that the majority of channels are closed in the absence of stimulation. Mechanical stimulation, known to mobilize Cx43-mediated channels in astrocytes (Stout et al., 2002), elicited a substantial increase in transmembrane dye influx that could be inhibited by the dual-specificity chloride channel/connexin-mediated hemichannel inhibitor FFA and was not affected by the chloride channel inhibitor DIDS. Recent studies have

reported that Cx43 hemichannels control Ca^{2+} intercellular signaling in cultured astrocytes through the release of adenosine triphosphate (Stout et al., 2002) and mediate bisphosphate-induced antiapoptotic signaling in osteocytes (Plotkin et al., 2002). Our data are consistent with these reports as well as providing the first evidence of dye influx in neural progenitors.

In summary, this study demonstrates that differential expression of Cx30, Cx36, Cx37, Cx43, and Cx46.6 is associated with differentiation of human NT2/D1 progenitors to hNT neurons and NT-G nonneuronal cells. Our data indicate that NT2/D1 progenitors can form functional gap junctions and inducible hemichannels in nonjunctional membranes and that this capacity is reduced significantly following terminal differentiation.

ACKNOWLEDGMENTS

We gratefully acknowledge the technical assistance of Jim Bennett. This study was supported by the Natural Sciences and Engineering Research Council of Canada (NSERC), Premier's Research Excellence Award, and Ontario Mental Health Intermediate Investigator Fellowship to S.A.L.B. S.B. is supported by an NSERC graduate studentship.

REFERENCES

Altevogt BM, Kleopas A, Postma FR, Scherer SS, Paul DL. 2002. Connexin29 is uniquely distributed within myelinating glial cells of the central and peripheral nervous system. J Neurosci 22:6458–6470.

Andrews PW, Damjanov I, Simon D, Banting GS, Carlin C, Dracopoli NC, Fogh J. 1984. Pluripotent embryonal carcinoma clones derived from the human teratocarcinoma cell line Tera-2. Lab Invest 50:147–162.

Baker KA, Hong M, Sadi D, Mendez I. 2000. Intrastriatal and intranigral grafting of hNT neurons in the 6-OHDA rat model of Parkinson's disease. Exp Neurol 162:350–360.

Baldassarre G, Boccia A, Bruni P, Sandomenico C, Barone MV, Pepe S, Angrisano T, Belletti B, Motti ML, Fusco A, Viglietto G. 2000. Retinoic acid induces neuronal differentiation of embryonal carcinoma cells by reducing proteasome-dependent proteolysis of the cyclin-dependent inhibitor p27. Cell Growth Differ 11:517–526.

Bani-Yaghoub M, Bechberger JF, Naus CCG. 1997. Reduction of connexin43 expression and dye-coupling during neuronal differentiation of human NTera2/Clone D1 Cells. J Neurosci Res 49:19–31.

Bani-Yaghoub M, Underhill TM, Naus CC. 1999a. Gap junction blockage interferes with neuronal and astroglial differentiation of mouse P19 embryonal carcinoma cells. Dev Genet 24:69–81.

Bani-Yaghoub M, Felker JM, Naus CC. 1999b. Human NT2/D1 cells differentiate into functional astrocytes. Neuroreport 10:3843–3846.

Bani-Yaghoub M, Bechberger JF, Underhill TM, Naus CCG. 1999c. The effects of gap junction blockage on neuronal differentiation of human NTera2/Clone D1 cell. Exp Neurol 156:16–32.

Bennett SAL, Chen J, Pappas BA, Roberts DCS, Tenniswood M. 1998. Alterations in platelet activating factor receptor expression associated with neuronal apoptosis in an in vivo model of excitotoxicity. Cell Death Differ 5:867–875.

Bennett SAL, Pappas BA, Stevens WD, Davidson CM, Fortin T, Chen J. 2000. Cleavage of amyloid precursor protein elicited by chronic cerebral hypoperfusion. Neurobiol Aging 21:207–214.

Bittman KS, LoTurco JJ. 1999. Differential regulation of connexin 26 and 43 in murine neocortical precursors. Cereb Cortex 9:188–195.

Bittman K, Owens DF, Kriegstein AR, LoTurco JJ. 1997. Cell coupling and uncoupling in the ventricular zone of the developing neocortex. J Neurosci 17:7037–7044.

Bruzzone R, White TW, Paul DL. 1996. Connections with connexins: the molecular basis of direct intercellular signaling. Eur J Biochem 238:1–27.

Castro C, Gomez-Hernandez JM, Silander K, Barrio LC. 1999. Altered formation of hemichannels and gap junction channels caused by C-terminal connexin-32 mutations. J Neurosci 19:3752–3760.

Crain B, Cotman C, Taylor D, Lynch G. 1973. A quantitative electron microscopic study of synaptogenesis in the dentate gyrus of the rat. Brain Res 63:195–204.

Dermietzel R, Spray DC. 1993. Gap junctions in the brain: where, what type, how many and why? Trends Neurosci 16:186–192.

Duffy HS, John GR, Lee SC, Brosnan CF, Spray DC. 2000. Reciprocal regulation of the junctional proteins claudin-1 and connexin43 by interleukin-1beta in primary human fetal astrocytes. J Neurosci 20: RC114.

Duval N, Gomes D, Calaora V, Calabrese A, Mead P, Bruzzone R. 2002. Cell coupling and Cx43 expression in embryonic mouse neural progenitor cells. J Cell Sci 115:3241–3251.

Ferrari A, Ehler E, Nitsch RM, Gotz J. 2000. Immature human NT2 cells grafted into mouse brain differentiate into neuronal and glial cell types. FEBS Lett 486:121–125.

Fulton BP. 1995. Gap junctions in the developing nervous system. Perspect Dev Neurobiol 12:327–334.

Gage FH. 2000. Mammalian neural stem cells. Science 267:1433–1438.

Garbuzova-Davis S, Willing AE, Milliken M, Saporta S, Zigova T, Cahill DW, Sanberg PR. 2002. Positive effect of transplantation of hNT neurons (NTera 2/D1 cell-line) in a model of familial amyotrophic lateral sclerosis. Exp Neurol 174:169–180.

Guthrie SC, Gilula NB. 1989. Gap junctional communication and development. Trends Neurosci 12:12–16.

Harris AL. 2001. Emerging issues of connexin channels: biophysics fills the gap. Q Rev Biophys 34:325–472.

Hurlbert MS, Gianani RI, Hutt C, Freed CR, Kaddis FG. 1999. Neural transplantation of hNT neurons for Huntington's disease. Cell Transplant 8:143–151.

Kammermans M, Fahrenfort I, Schultz K, Janssen-Bienhold U, Sjoerdsma T, Weiler R. 2001. Hemichannel-mediated inhibition in the outer retina. Science 292:1178–1180.

Larson DM, Seul KH, Berthoud VM, Lau AF, Sagar GD, Beyer EC. 2000. Functional expression and biochemical characterization of an epitope-tagged connexin37. Mol Cell Biol Res Commun 3:115–121.

Lo Turco JJ, Kriegstein AR. 1991. Clusters of coupled neutralists in embryonic neocortex. Science 252:563–566.

Meltzer CC, Kondziolka D, Villemagne VL, Wechsler L, Goldstein S, Thurlborn KR, Gebel J, Elder EM, DeCesare S, Jacobs S. 2001. Serial [^{18}F]fluorodeoxyglucose positron emission topography after human neuronal implantation for stroke. Neurosurgery 49:586–591.

Mercier F, Hatton GL. 2001. Connexin 26 and basic fibroblast growth factor are expressed primarily in the suppial and subependymal layers in adult brain parenchyma: roles in stem cell proliferation and morphological plasticity? J Comp Neurol 431:88–104.

Nadarajah B, Jones AM, Evans WH, Parnavelas JG. 1997. Differential expression of connexins during neocortical development and neuronal circuit formation. J Neurosci 17:3096–3111.

Nagy JI, Li X, Rempel J, Stelmack G, Patel D, Staines WA, Yasumaura T, Rash JE. 2001. Connexin26 in adult rodent central nervous system: demonstration at astrocytic gap junctions and colocalization with connexin30 and connexin43. J Comp Neurol 441:302–323.

Nelson PT, Kondziolka D, Wechsler L, Goldstein S, Gebel J, Decesare S, Elder EM, Zhang PJ, Jacobs A, McGrogan M, Lee VM, Trojanowski JO. 2002. Clonal human (hNT) neuron grafts for stroke therapy: neuropathology in a patient 27 months after implantation. Am J Pathol 160:1201–1206.

Peinado A. 2001. Immature neocortical neurons exist as extensive syncitial networks linked by dendrodendritic electrical connections. J Neurophysiol 85:620–629.

Peinado A, Yester R, Katz LC. 1993a. Extensive dye coupling between rat neocortical neurons during the period of circuit formation. Neuron 10:103–114.

Peinado A, Yuste R, Katz LC. 1993b. Gap junctional communication and the development of local circuits in neocortex. Cereb Cortex 3:488–498.

Pleasure SJ, Page C, Lee VM-Y. 1992. Pure, post mitotic, polarized human neurons derived from NTera 2 cells provide a system for expressing exogenous proteins in terminally differentiated neurons. J Neurosci 12: 1802–1815.

Plotkin LI, Manolagas SC, Bellido T. 2002. Transduction of cell survival signals by connexin-43 hemichannels. J Biol Chem 277:8648–8657.

Rash JE, Staines WA, Yasumura T, Patel D, Furman CS, Stelmack GL, Nagy JL. 2000. Immunogold evidence that neuronal gap junctions in adult rat brain and spinal cord contain connexin-36 but not connexin-32 or connexin-43. Proc Natl Acad Sci USA 97:7573–7578.

Rash JE, Yasumura T, Davidson KG, Furman CS, Dudek FE, Nagy JL. 2001. Identification of cells expressing Cx43, Cx30, Cx26, Cx32 and Cx36 in gap junctions of rat brain and spinal cord. Cell Adhes Commun 8:315–320.

Rozental R, Morales M, Mehler MF, Urban M, Kremer M, Dermeitzel R, Kessler JA, Spray DC. 1998. Changes in the properties of gap junctions during neuronal differentiation of hippocampal progenitor cells. J Neurosci 18:1753–1762.

Rozental R, Srinivas M, Gokhan S, Urban M, Dermietzel R, Kessler JA, Spray DC, Mehler MF. 2000. Temporal expression of neuronal connexins during hippocampal ontogeny. Brain Res Brain Res Rev 32:57–71.

Sandhu JK, Sikorska M, Walker PR. 2002. Characterization of astrocytes derived from human NTera-2/D1 embryonal carcinoma cells. J Neurosci Res 68:604–612.

Saporta S, Willing AE, Zigova T, Daadi MM, Sanberg PR. 2001. Comparison of calcium-binding proteins expressed in cultured hNT neurons and hNT neurons transplanted into the rat striatum. Exp Neurol 167:252–259.

Sodja C, Fang H, Dasgupta T, Ribecco M, Walker PR, Sikorska M. 2002. Identification of functional dopamine receptors in human teratocarcinoma NT2 cells. Brain Res Mol Brain Res 99:83–91.

Srinivas M, Rozental R, Kojima T, Dermietzel R, Mehler M, Condorelli DF, Kessler JA, Spray DC. 1999. Functional properties of channels formed by the neuronal gap junction protein connexin36. J Neurosci 19:9848–9855.

Stout CE, Costantin JL, Naus CC, Charles AC. 2002. Intercellular calcium signaling in astrocytes via ATP release through connexin hemichannels. J Biol Chem 22:10482–10488.

Temple S. 2001. The development of neural stem cells. Nature 414:112–117.

Teubner B, Degen J, Sohl G, Guldenagel M, Bukauskas FF, Trexler EB, Verselis VK, De Zeeuw CI, Lee CG, Kozak CA, Petrasch-Parwez E, Dermietzel R, Willecke K. 2000. Functional expression of the murine connexin 36 gene coding for a neuron-specific gap junctional protein. J Membrane Biol 176:249–262.

Teubner B, Odermatt B, Guldenagel M, Sohl G, Degen J, Bukauskas F, Kronengold J, Verselis VK, Jung YT, Kozak CA, Schilling K, Willecke K. 2001. Functional expression of the new gap junction gene connexin47 transcribed in mouse brain and spinal cord neurons. J Neurosci 21:1117–11126.

Traub O, Hertlein B, Kasper M, Eckert R, Krisciukaitis A, Hulser D, Willecke K. 1998. Characterization of the gap junction protein connexin37 in murine endothelium, respiratory epithelium, and after transfection in human HeLa cells. Eur J Cell Biol 77:313–322.

Valiunas V. 2002. Biophysical properties of connexin-45 gap junction hemichannels studies in vertebrate cells. J Gen Physiol 119:147–164.

Willecke K, Eiberger J, Degen J, Eckardt D, Romualdi A, Guldenagel M, Deutsch U, Sohl G. 2001. Structural and functional diversity of connexin genes in the mouse and human genome. Biol Chem 383:725–737.

Willing AE, Garbuzova-Davis S, Saporta S, Milliken M, Cahill DW, Sanberg PR. 2001. hNT neurons delay onset of motor deficits in a model of amyotrophic lateral sclerosis. Brain Res Bull 56:525–530.